Synthesis, Characterization and Antimicrobial Activity of Cu(II), Co(II), Ni(II), Pd(II) and Ru(III) Complexes with Clomiphene Citrate

KS Prasad[1], LS Kumar[1], HD Revanasiddappa[1]*, B Vijay[2], B Jayalakshmi[3]

[1]Department of Chemistry, University of Mysore, Manasagangothri, Mysore-570 006, India.
[2]Department of Chemistry, University of BDT College of Engineering, Davanagere University, Davanagere-577 004, India.
[3]Department of Botany, Maharani's Science College for Women, Mysore-570 006, India.

*Correspondence to: Hosakere D Revanasiddappa, hdrevanasiddappa@yahoo.com

Accepted: March 30, 2011; Published: June 27, 2011

Abstract

The new mononuclear neutral metal complexes of the type $[M(L)_2(H_2O)_nX_n]$ (where n= 0,1,2...; X= Cl; ½ SO_4; CH_3COO; Br) by using the metal(II/III) salts {M = Cu(II), Co(II), Ni(II), Pd(II) and Ru(III)} with the Clomiphene citrate (***L***) were synthesized. The ligand and its complexes were characterized by elemental analysis, infrared, ESR, ^{1}H-NMR, electronic spectral studies and magnetic susceptibility measurement, which reveals that ***L*** acts as a monodentate ligand. They simultaneously give Thermogravimetric and Differential Thermal Analysis patterns of the complexes recorded at heating rate of 10 °C min^{-1}. The antimicrobial activity of ligand and its metal complexes were evaluated against Gram positive and Gram negative bacteria.

Keywords: Transition metal complexes; clomiphene citrate; TG-DTA; antibacterial; antifungal activity.

1. Introduction

The chemistry of transition metal complexes has received much attention in recent years on account of their rational design and synthesis in coordination chemistry, also because of their potential applications as functional materials [1], enzymatic reaction mechanism [2] and in bioinorganic chemistry [3]. The transition metal complexes with nitrogen donors are applied in various activities such as anticancer, antitubercular, antibiotic, antimicrobial and antifungal agents [4, 5].

Clomiphene citrate (***L***), chemically (2-[4-(2-chloro-1, 2-diphenylethenyl)phenoxy]-*N,N*-diethyl ethanamine) is a biologically active compound having vinyl aryl group to which an alkylic chain is attached with a donor nitrogen atom, thus making a cavity to bind the metal ion. Clomiphene citrate (***L***) inhibits the negative feedback mechanism, which suppresses release of gonadotropins-releasing hormone and gonadotropins themselves [6, 7]. Its synergistic effects are in induction of ovulation. Sorbie and Perez-Marrero [8] have studied its use in male infertility. HPLC method [9] for the determination of its isomers in human plasma is also reported. A detailed survey of literature reveals that coordination chemistry of metal complexes with ***L*** has not been carried out yet.

Synthesis of dinuclear complexes using the bidentate ligands has been carried out by many authors [10, 11].Many of the metals has found widespread application in organic synthesis and biology [12, 13]. Currently, the use of such metal complexes is promising since they act as single-molecule magnets (SMMs) [14], as luminescent probes [15], as catalysts for specific DNA [16] and RNA [17] cleavage reactions and some transition metal complexes (M¼Cu, Co, Ni, etc.) of Schiff base ligands with the potent inhibitory activities against urease have also been reported by us [18]. Palladium (Pd) compounds provide useful catalysts for organic transformations to produce a wide range of organic compounds such as pharmaceuticals, agrochemicals, and organic materials for various applications [19, 20]. Organopalladium compounds, typical intermediates in Pd-catalyzed organic transformations, generally prefer low formal oxidation states such as 0 and +2. Due to these important applications, we became interested in the synthesis of Pd(II) and Ru(III) complexes of biologically potent 2-[4-(2-chloro-1, 2-diphenylethenyl)phenoxy]-*N,N*-diethyl ethanamine.

The aim of the present study is to synthesize copper(II)(***1a-1c***), cobalt(II) (***2a-2d***), nickel(II) (***3a-3c***), palladium(II) (***4a***) and ruthenium(III) (***5a***) complexes with clomiphene citrate ***(L)*** as the ligand. The data obtained by elemental analysis, spectroscopic, magnetic and thermal studies were correlated and used to elucidate the structural formulae of the prepared complexes. Apart from this, the biological efficacy of the metal complexes was studied against few bacteria and fungi.

2. Methods

2.1. Materials

Clomiphene citrate was received from Cipla Ltd., India and used as such. Among the solvents employed, dimethyl formamide (DMF) and dimethyl sulfoxide (DMSO) were of spectroscopic grade and remaining solvents were of AR grade purchased from commercial source. The commercial ethanol sample was refluxed over calcium oxide for 6 h, distilled and used.

2.2. Instrumentation

Infrared spectral measurements for the free ligand and its metal complexes were recorded in KBR pellets using a Jasco FT-IR 4100 type double beam spectrophotometer. EPR spectra were recorded on a Varian E-12 spectrometer equipped with a HP-5342A frequency meter and Bruker NMR gaussmeter. The ESR studies were performed by using a spectroelectrochemical cell. ^{1}H-NMR spectra were taken for the ligand and its complexes using AMX-400 FT-NMR spectrophotometer. The ^{1}H-NMR spectra were recorded employing TMS as a reference and DMSO-d_6 as a solvent at ambient temperature. Elemental analysis data (C, H, N) were obtained with a Elementarvario EL-III instrument. Electronic spectra of the complexes in the UV-visible region (200-900 nm) were measured using a Jasco UVIDEC-610 double beam spectrophotometer with quartz cells.

2.3. Synthesis of metal complexes

2.3.1. General procedure for the synthesis of 1a-1c, 2a-2d, 3a-3c, 4a and 5a {**(a)**Cl; (**b**) CH_3COO; **(c)** ½ SO_4; (**d**) Br**}**

A hot ethanol solution of ***L*** (2.99g, 5 mmol, 30 mL) was slowly added to each 15 mL of 2.5 mmol hot ethanol solution of respective metal salt with continuous stirring. The reaction mixture was refluxed for 4 h. The colored precipitates obtained in each case after cooling to room temperature was filtered off, washed several times with ethanol and then with ether, finally dried in an evacuated desiccator over anhydrous silica gel. Sulphate complexes were prepared in aqueous media.

2.3.2. Molar conductance and magnetic susceptibility measurements

The conductance data were recorded in 10^{-4} M DMF solution at room temperature using an Elico CM-180 conductometer. The cell constant of the conductivity cell used was 0.5 cm^{-1}. The magnetic susceptibility measurements of the complexes were carried out by using Gouy method at room temperature. The effective magnetic moment per metal atom was calculated from the expression,

$$\mu_{eff} = 2.84\ [\chi_m\ T]^{1/2}\ B.M$$

where χ_m is the molar susceptibility of the complex obtained after applying the diamagnetic corrections by the use of Pascal's constant for other atoms and groups in the complex. $Hg[Co(SCN)_4]$ was used as a calibrant.

2.3.3. Thermal analyses

Thermal analyses of the complexes were recorded on a Perkin Elmer, US TGA-7 analyzer in the atmosphere of air. The temperature scale of the instrument was calibrated with high purity calcium oxalate. The operational range of the instrument was from ambient to 900 °C. Accurately 5 mg of pure sample was subjected for dynamic TG scans at heating rate of 10 °C min^{-1}.

2.4. Antibacterial activity

Antibacterial activity of the ligand and its complexes was determined against*E.coli*MTCC443, *Staphylococcus aureus*MTCC737, *Ralstoniasolanacearum* NCIM5103 (NCL, Pune)and *Xanthomonas vesicatoria*(Danida lab, UOM, Mysore) by Disk diffusion method [21]. The pure cultures of these organisms were obtained from the Department of Biotechnology, Bapuji Institute of Engineering and Technology, Davangere. The organisms used in the compounds were sub-cultured into sterile nutrient broth. After incubating the same at 37 °C for 3 h, the growth thus obtained was used as inoculums for the tests. Nutrient agar (28 gL^{-1}) and nutrient broth were sterilized in conical flask of suitable capacity by autoclaving at 15 lb pressure for 30 min. The agar medium was melted on water bath and cooled to 45 °C. To the 20 to 25 mL molten agar 0.5 to 0.7 mL of 3 h old sub-culture was added aseptically, mixed well by gentle shaking and allowed to attain room temperature in Petri dishes.

The sterilized filter paper disks (Whatmann 41) were loaded with known volume of the test compound of known strength using micropipette, to get the disk of desired concentration. The disks are placed over the growth media seeded with microorganisms, left for diffusion and incubated at 37 ± 2 °C for 24 h. The experiment is carried out with four replicates for each concentration. The antibiotic Chloramphenicol was also screened under similar conditions for comparison as a standard and the solvent DMSO was also put to know the activity.

2.5. Antifungal activity

Antifungal activity of the test compounds was determined against two fungi,*A. flavus*and *A. niger*,by Batemann poisoned food technique [22]. These fungi were cultured for seven days on Czapek's agar in sterilized petri dishes under 12/12 h light and darkness. The ligand and its metal complexes dissolved in DMSO were added to 10-15 mL of sterilized media to achieve different concentrations at 35 ± 2 °C and allowed the media for solidification. The test fungi were taken as 2 mm disks from 10 days old pure colonies and placed in the petri plates containing Czapek's agar nutritive medium. The experiments were carried out in four replicates per treatment and incubation was carried out at 22 ± 2 °C under 12/12 light and darkness. The radical growth of the colony was recorded after 96 h of incubation.

3. Results and Discussion

To design novel structures of metal complexes, the ligand used in the preparation is important. In this article, the author synthesized the complexes (as shown in Figure 3) in such a way that ligand ***L***could coordinate to the metal ions through the alkylic nitrogen atom. In this work, all complexes were synthesized using the same synthetic procedure and exhibit octahedral geometry except palladium complexes, instead giving square planar geometry.

All the complexes are soluble in most polar organic solvents, such as DMSO and DMF. The elemental analyses are in good agreement with the chemical formulae proposed for the compounds and spectral techniques *viz.*^{1}H-NMR, IR, electronic spectra and thermal studies provided evidence for the proposed structures.

3.1. Molarconductance and magnetic susceptibility

The molar conductance data of the complexes in DMF at 10^{-3} M are presented in Table 1. The molar conductance values lie in the range 12.7 – 30.7 Ohm^{-1} cm^{2} mol^{-1} which indicates that the anions are coordinated to the central metal ion. The slightly higher values than those expected for non-electrolytes in these cases are probably due to partial replacement of the anion by the strong donor solvent molecule and the two species may exist in equilibrium. Further, dissociation of coordinated halides in DMF leading to substantially high conductance has been reported in literature [23, 24]. Therefore, the complexes may perhaps be considered as non-electrolytes.

Table 1: Analytical and physical data of the metal complexes.

Compounds	M %		C %		H %		N %		Molar Conductance Ω-1 cm2M-1	μeff(BM)
	Obsd	Calcd	Obsd	Calcd	Obsd	Calcd	Obsd	Calcd		
1a	6.38	6.47	63.39	63.60	6.12	6.11	2.77	2.85	18.7	1.86
1b	6.14	6.17	65.22	65.36	6.39	6.41	2.69	2.72	19.4	1.89
1c	6.25	6.31	61.7	62.02	5.93	5.95	2.79	2.78	21.1	1.94
2a	5.93	6.02	63.63	63.81	6.13	6.17	2.86	2.93	17.5	4.92
2b	5.76	5.77	65.51	65.66	6.42	6.44	2.68	2.73	18.2	5.24
2c	5.73	5.87	62.07	62.31	5.95	5.98	2.77	2.79	17.9	4.32
2d	5.53	5.52	58.17	58.49	5.59	5.62	2.83	2.86	19.7	4.89
3a	5.98	6.01	63.79	63.89	6.12	6.13	2.83	2.86	18.7	3.21
3b	5.62	5.72	65.23	65.58	6.43	6.44	2.70	2.73	19.4	3.36
3c	5.81	5.85	61.99	62.23	5.96	5.98	2.75	2.79	14.1	3.18
4a	10.57	10.75	62.86	63.07	5.65	5.66	2.80	2.83	23.5	Dia
5a	6.38	6.47	63.39	63.60	6.12	6.11	2.77	2.85	18.7	1.86

Dia = Diamagnetic; Obsd = Observed; Calcd = Calculated.

Among the studied complexes ***4a*** is found to be diamagnetic thus suggesting square planar arrangement of the ligand molecules around the central metal ion. At room temperature, the magnetic moments of remaining complexes were lies in the range 1.79 to 5.24 BM (Table 1). The lowering in magnetic moment may arise due to lower symmetry ligand fields or electron delocalization [25] and suggests the low spin $d^5(t_{2g}^5)$ configuration in an octahedral environment. The magnetic properties of high spin octahedral complexes are governed by the orbital degenerate ground term $^4T_{1g}$, which arise from the $t_{2g}^5 e_g^2$ configuration.

3.2. ESR spectral studies

The ESR study is useful in understanding the geometry and state of electrons in metal ion of the complexes. In the present study, the ESR spectra of the Cu(II) complexes is recorded in a DMSO solution and related parameters are given in Table 2. The solid-state ESR spectra of some of the complexes exhibit axially symmetric g-tensor parameters with $g_{||} > g_{\perp} > 2.0023$, indicating that the copper site has a $d_{x^2-y^2}$ ground-state characteristic of tetrahedral, square-planar, or octahedral stereochemistry. The $g_{||} > g_{\perp}$ for synthesized Cu(II) complexes, ***1a*** and ***1c*** indicates a tetragonal distortion. In axial symmetry, the G-values are given by Eq. 1.

$$G = (g_{||} - 2)/(g_{\perp} - 2) = 4 \quad \rightarrow (1)$$

where G is the exchange interaction parameter, according to literature, for the considerable exchange interaction process between Cu(II) centers in the solid state the value of $G \leq 4$. The G values obtained for Cu(II) complexes, ***1a*** and ***1c*** are 2.11 and 2.08, respectively, which satisfy the above mentioned parameter. The g_{av} values were

evaluated by using the relation $g_{av} = 1/3\ g_{||} + 2/3\ g_{\perp}$, and these calculated values are in agreement with an orbital non-degenerate state [26].

Table 2: ESR data of Copper(II) complexes in DMSO.

Complex	$g_{\parallel}$	$g_{\perp}$	G	g_{av}
1a	2.2369	2.1643	2.1146	2.0826
1c	2.1645	2.1548	2.0871	2.0718

3.3. Infrared spectra

The IR spectral data of ***L*** and its complexes are given in Table 3. The far IR spectra of the complexes provide a sharp band at 320-385 cm^{-1} and at 425-440 cm^{-1} are assigned to υ(M-X) (X=halide) and υ(M-N), respectively. Therefore, the IR spectra of ***L*** and its complexes show that ligand acts as a monodentate donor atom by coordination through the quaternary nitrogen attached to alkyl group. In the spectra of all complexes, a broad band at 3500-3300 cm^{-1} may be assigned to υ(OH) of the coordinated water [27].

Table 3: IR data of ***L*** and its complexes (in cm^{-1}).

Compounds	υ(OH)	υ(C-O-C)	υ(M-N)	υ(M-halide)
L	-	1150	-	-
1a-1c	3469-3460	1150	432-426	366-323
2a-2d	3353-3313	1150	440-432	363-329
3a-3c	3496-3302	1150	439-425	381-372
4a	-	1150	430	385
5a	-	1150	429	357

3.4. ^{1}H-NMR spectra

The ^{1}H-NMR spectra of ***L*** and its complex of Pd(II) salt were discussed in this section. The ^{1}H-NMR spectra of ***L*** exhibits a signal at δ 1.0 ppm and one multiplet centered around at δ 7.0 ppm are assigned to alkyl and aromatic protons, respectively. A sharp signal (singlet) at δ 2.78 ppm is due to tertiary nitrogen attached to the alkyl group. In the ^{1}H-NMR spectra of the Pd(II) complex (4a), resonance at δ 1.0 ppm and δ 7.0 ppm were in the same position as in the free ligand, but the signal around δ 2.96 ppm indicate a downfield shift of alkyl protons attached to the tertiary nitrogen, thereby suggesting the involvement of tertiary nitrogen atom in coordination with metal ions.

3.5. Electronic spectra

The electronic spectra of ***1a-1c*** complexes display two bands in the visible region, one at 10260-11300 cm^{-1} being assigned to $^2B_{1g} \rightarrow {}^2A_{1g}$ and $^2B_{1g} \rightarrow {}^2B_{2g}$ transitions, while the second band around 18340-22788 cm^{-1} attributed to $^2B_{1g} \rightarrow {}^2E_g$ transitions suggesting a distorted octahedral configuration [28]. The solution of ***2a – 2d*** exhibit three d-d transition, one in the region 14390-14530 cm^{-1} which is assigned to $^4T_{1g}(F) \rightarrow {}^4T_{2g}$ (F) (υ_1) having high spin octahedral geometry, another at 14850 cm^{-1} is assigned to $^4T_{1g}$ (F) $\rightarrow {}^4A_{2g}$ (F) (υ_2) which in some cases not observed at all, but the fine structure arises due to symmetry. Third transition occurs at 16430 cm^{-1} is attributed to $^4T_{1g}$ (F) $\rightarrow {}^4T_{1g}$ (P) (υ_3). The more intense bands beyond 36500 cm^{-1} are charge transfer bands. The ***3a-3c***also show two bands in the region 12830-16380 cm^{-1} due to $^4A_{2g} \rightarrow {}^3T_{1g}$ (F) and $^4A_{2g} \rightarrow {}^3T_{1g}$ (P) transition. An intense band at ~30000 cm^{-1} corresponds to intra ligand charge transfer transition within the ligand which are assigned to $n \rightarrow \pi^*$ transitions. The facts accompanied by magnetic moment and electronic spectra of ***1a-1c, 2a-2d*** and ***3a-3c*** complexes suggest an octahedral arrangement.The ground state for low-spin Pd(II) ion is $^1A_{1g}(a_{1g}^2, e_g^4, b_{2g}^2)$.The electronic spectra of ***4a***show a broad bandin the region 22222-23000 cm^{-1} which is assigned to $^1A_{1g} \rightarrow {}^1B_{1g}$ transition. This transition is a characteristic of square planar palladium complexes, while ***5a***showed only charge

transfer bands which masked the weak (spin forbidden as well as spin allowed) bands due to d-d transitions in the visible region. The band in the range 25000-27120 cm^{-1} may be assigned to $^1A_{1g} \rightarrow {}^1T_{2g}$ and charge transfer transition [33]. The bands in the range 34480-37045 cm^{-1} can be assigned to $\pi \rightarrow \pi^*$ transitions. Thus, the ***5a*** is attributed to octahedral stereochemistry.

3.6. Thermogravimetric analyses

The TGA and DTA curves show three decomposition steps for all complexes except ***4a*****,** which decompose in two steps. In the three stepdecomposition, first degradation step occurs at the temperature range 128-245 °C corresponds to the loss of two coordinated water molecules. The major weight loss occurs in second thermal decomposition step at the temperature range 195–416 °C, this weight loss corresponds to the expulsion of two molecules of ***L*****,** while in ***5a*** this step occurs at 205–426 °C (Table 4). The third thermal decomposition step occurs in the temperature range 305–640 °C corresponds to the loss of coordinated inorganic ligands. The final residue of the decomposition at above 640 °C corresponds to metal(II) oxide, which is in conformity with the observed and calculated weights of pyrolysis products. The ***4a*** is stable up to 224 °C, and then it undergoes decomposition in two stages. The first degradation step occurs at the temperature range 225-425 °C corresponds to the loss of two molecules of ***L***. The second degradation step occurs at the temperature range 450-640 °C which corresponds to the loss of coordinated inorganic ligand chloride. The percentage weight losses lie in the calculated range.

Table 4: Stepwise thermal degradation data obtained from TGA curves.

Complex	Temp. range (°C)	Degradation of products	% Weight loss		No. of moles	% Residue (z)	
			Calcd.	Expt.		Calcd.	Expt.
(1a)	174-218 240-286 310-580	2 H_2O 2 ***L*** 2 Cl	3.66 82.65 7.21	3.14 80.56 6.92	2 2 2	8.09	7.90
(1b)	170-210 240-350 380-640	2 H_2O 2 ***L*** SO4	3.57 80.59 9.52	3.18 78.95 8.76	2 2 1	7.89	7.33
(1c)	128-185 212-265 306-400	2 H_2O 2 ***L*** 2 ac	3.49 78.86 11.46	3.06 76.68 10.66	2 2 2	7.27	7.27
(2a)	190-245 260-410 430-620	2 H_2O 2 ***L*** 2 Cl	3.68 83.04 7.25	3.89 81.40 6.52	2 2 2	7.66	6.34
(2b)	140-190 215-330 360-620	2 H_2O 2 ***L*** SO_4	3.58 80.96 6,41	3.20 78.69 5.77	2 2 1	7.47	6.74
(2c)	122-180 200-330 340-580	2 H_2O 2 ***L*** 2 ac	3.51 79.22 11.51	3.18 79.29 10.83	2 2 2	7.31	6.92
(2d)	176-225 229-350 370-555	2 H_2O 2 ***L*** 2 Br	3.37 76.11 14.98	3.00 74.56 13.89	2 2 2	7.02	6.82
(3a)	126-192 210-265 495-560	2 H_2O 2 ***L*** 2 Cl	3.68 83.06 7.25	3.18 79.45 6.68	2 2 2	7.64	6.46
(3b)	132-188 198-356 426-534	2 H_2O 2 ***L*** SO_4	3.60 80.98 9.57	3.25 76.88 8.29	2 2 1	7.44	6.85
(3c)	116-178 195-290 330-540	2 H_2O 2 ***L*** 2 ac	3.51 79.29 11.23	3.00 76.45 10.86	2 2 2	11.46	10.69
(4a)	225-425 450-640	2 ***L*** 2 Cl	82.7 7.16	79.92 6.85	2 2	12.37	11.03
(5a)	168-202 205-426 430-605	H_2O 2 ***L*** 3 Cl	1.73 78.27 10.25	2.43 76.15 9.22	1 2 3	12.04	10.92

L = Clomiphene citrate; ac = CH_3COO.

3.7. Antimicrobial studies

The *in vitro* antimicrobial screening effects of the ligand and its complexes were performed against bacteria *viz., S.aureus, E.coli, R.solanacearum*and *X.vesicatoria* by the disk diffusion method and against fungi *viz., A.flavus* and *A.niger* by Batemann poisoned food technique. The activities of the compounds were compared with those of standards such as Chloramphenicol for antibacterial and Griseoflavin for antifungal activity. Since DMSO was used as a solvent, it was also screened against all organisms and no activity was found.The antimicrobial properties of the ***L*** and its corresponding complexes are characterized determining the minimum inhibitory concentration (MIC), represented in Figure 1 and Figure 2. As the MIC on the basis of mass, the results presented in Table 5 and Table 6 indicates that the compounds have both antibacterial and antifungal activities against the tested organisms. At30 µg concentration the inhibition was very low compared to 60 µg concentration. It shows that as the concentration of the complexes increases, the inhibition of bacterial and fungal growth also increases. At 60 µg concentration for a given metal ion, chloro, bromo, sulphate and acetate complexes are having the antimicrobial activity in the order, acetate complex >sulphate complex >bromo complex >chloro complex. This indicates that in addition to nature of metal ions, the nature of anion in the complex play significant role in antimicrobial activities. This would suggest that the chelation could facilitate the ability of a complex to cross a cell membrane and can be explained by Tweedy's chelation theory [29]. All the test compounds show lesser activity than the standard antibiotics.

Table5: Antibacterial activity of ***L*** and its corresponding complexes, along with standard Chloramphenicol is presented as percentage inhibition.

Compound	Inhibition zone in mm							
	S. aureus		*E. coli*		*R.solanacearum*		*X.vesicatoria*	
	30 µg	60 µg	30 µg	60 µg	30 µg	60 µg	30 µg	60 µg
L	0	8	0	8	0	9	0	8
1a	8	14	8	16	8	14	8	15
1b	8	15	8	16	8	15	7	14
1c	8	19	8	16	8	16	8	17
2a	8	13	8	15	8	15	7	14
2b	8	14	9	17	8	14	8	13
2c	9	17	9	18	9	17	8	15
2d	8	16	9	17	10	17	8	14
3a	9	17	9	17	10	18	8	15
3b	10	18	10	17	10	19	9	16
3c	10	19	9	20	9	19	10	17
4a	10	20	12	22	11	21	11	20
5a	9	17	10	19	10	19	9	18
Chloramphenicol	25	44	30	52	28	54	27	50

DMSO showed no inhibition; each value is the average of four replicates.

Table6: Antifungal activity of ***L*** and its corresponding complexes, along with standard Griseofulvin is presented as percentage inhibition.

Compound	Percentage inhibition zone			
	A. flavus		*A. niger*	
	30 µg	60 µg	30 µg	60 µg
L	9	14	8	14
1a	22	48	27	54
1b	31	50	33	56
1c	33	57	33	60
2a	27	38	28	39
2b	31	35	29	37
2c	32	38	32	39
2d	30	36	29	38
3a	30	58	30	62
3b	29	63	30	60
3c	32	70	32	71
4a	34	72	31	70
5a	34	68	30	67
Griseofulvin	100	100	100	100

DMSO showed no inhibition; each value is the average of four replicates.

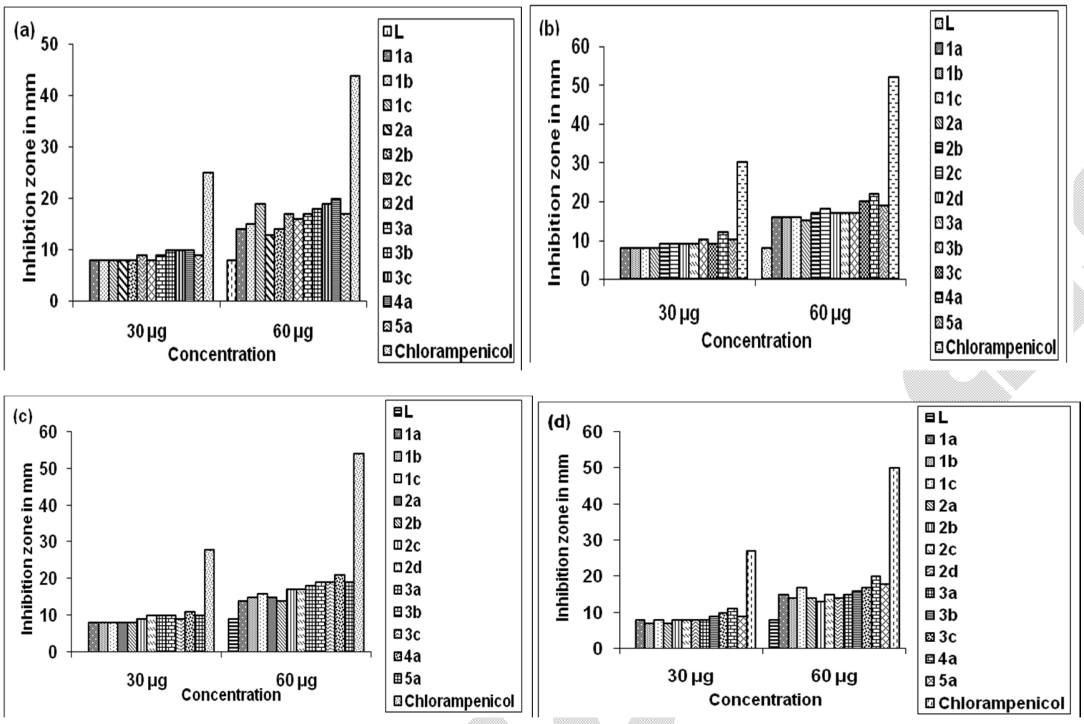

Figure 1: Representation of antibacterial activity of ligand and its complexes by inhibition zone in mm against, **(a)** *S. aureus*, **(b)** *E. coli*,**(c)** *P. aeraginosa*, **(d)** *B. subtilus*.

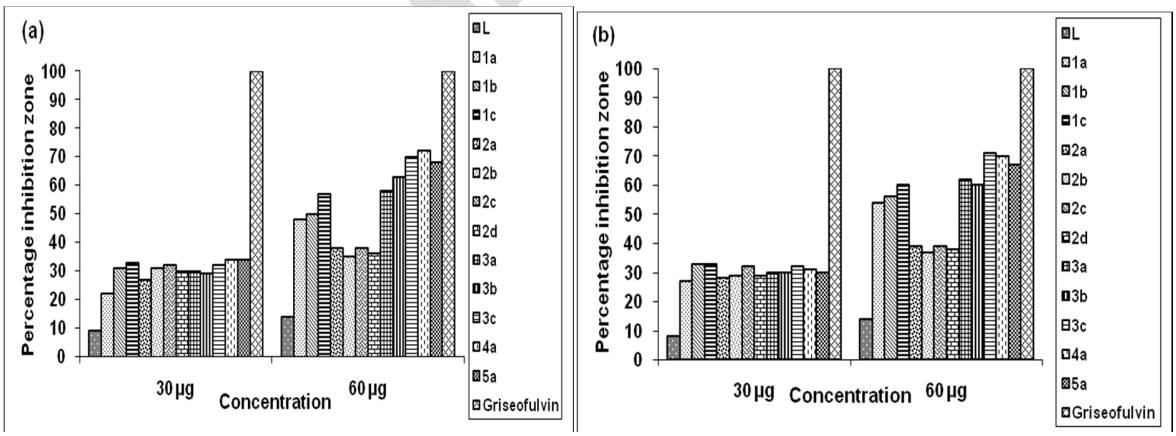

Figure 2: Representation of antifungal activity of ligand and its complexes by inhibition zone in mm against, **(a)** *A. flavus*, **(b)** *A. niger*.

4. Conclusion

The newly synthesized complexes were characterized using elemental analyses and spectroscopic methods. On the basis of spectral data, 1:2 stoichiometry was found for the metal:ligand. Non-electrolytic nature of the studied complexes showing the anions is coordinated to the central metal ion. The magnetic and electronic spectral studies support an octahedral geometry for all the complexes except ***4a*** which exhibit square planar geometry. Based on the spectral data the proposed geometries of the studied complexes are depicted in Figure 3. The results of *in-vitro* biocidal activities of the ligand and its metal complexes clearly show that the compounds have both antibacterial and antifungal potency against the tested organisms. The complexes showed more activity than free ligand.

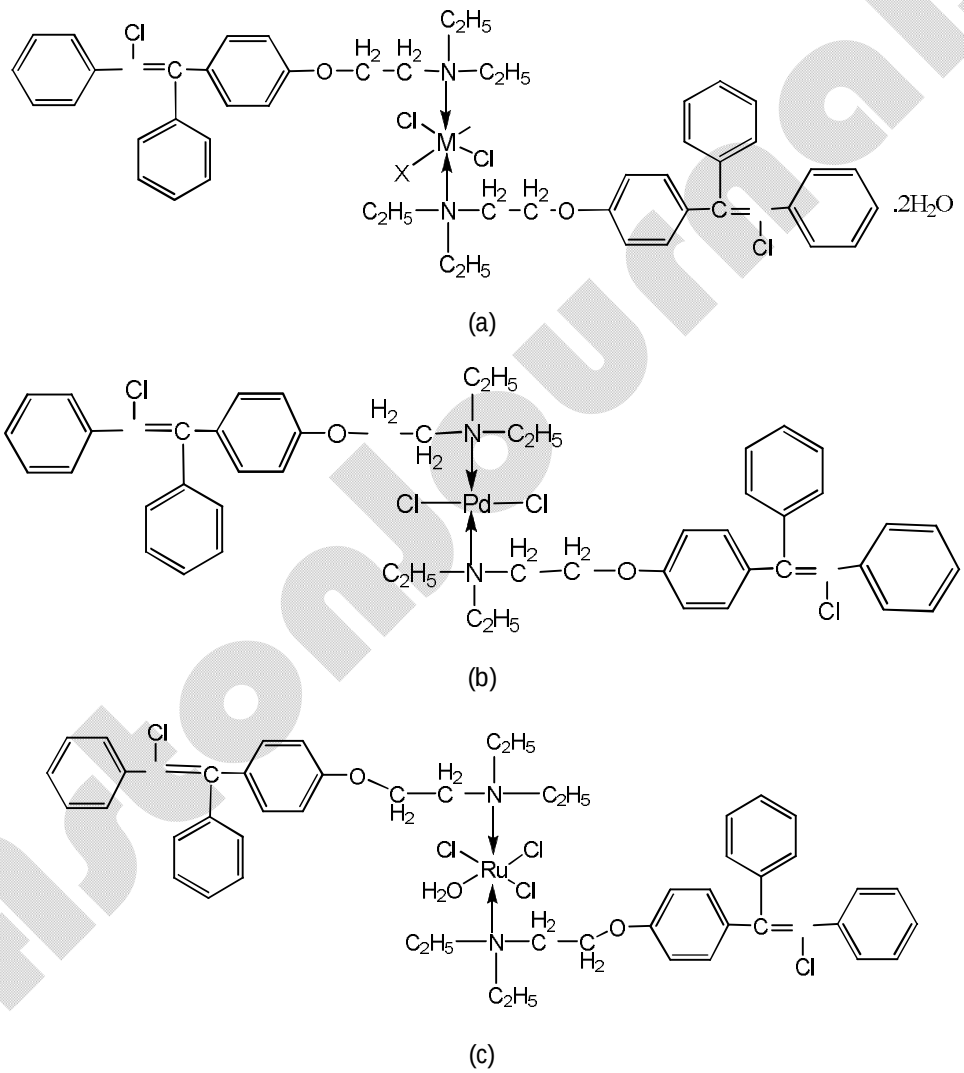

Figure 3: Suggested structure for (a) ***1a-1c, 2a-2d, 3a-3c*** [M= Cu(II), Co(II), Ni(II); X = Cl, CH_3COO, NO_3, ½ SO_4], (b) ***4a***, (c) ***5a***.

Competing Interests

The authors declare that they have no competing interests.

Authors' Contributions

KSP and LSK interpreted the analytical and spectral data and involved in the preparation of manuscript. BV carried out experimental work. BJ carried out biological studies and HDR reviewed the manuscript thoroughly.

Acknowledgement

The authors are thankful to the University of Mysore, Mysore for providing the laboratory facilities.

References

1. Radhakrishnan PK, Indrasenan P, Nair CGR, 1984. Complexes of lanthanide nitrates with 4n-(2′-hydroxy benzylidene)-aminoantipyrine. Polyhedron, 3: 67-70.
2. Maddi V, Raghu KS, Rao MNA, 1992. Synthesis and anti-inflammatory activity of 3-(Benzylideneamino) coumarins in rodents. Journal of Pharmaceutical Science, 81: 964-966.
3. Shail KC, Promod VP, Sonu CT, Tulsidas GS, 2005. Estradiol protects clomiphene citrate–induced apoptosis in ovarian follicular cells and ovulated cumulus–oocyte complexes. Fertility and Sterility, 84: 1163-1172.
4. Charles D, Turner JH, Redmond C, 2005. Karyotypicprofiles of women after clomiphene citrate therapy. International Journal of Obstetrics and Gynecology, 80: 264-270.
5. Sorbie PJ, Perez-Marrero R, 1984. Review article: The use of clomiphene citrate in male infertility. Journal of Urology, 131: 425–429.
6. Baustian CL, Mikkelson TJ, 1986. Analysis of clomiphene isomers in human plasma and detection of metabolites using reversed-phase chromatography and fluorescence detection. Journal of Pharmaceutical and Biomedical Analysis, 4: 237-246.
7. Gonzalez E, Rodrigue-Witchel A, Reber C, 2007. Absorption spectroscopy of octahedral nickel(II) complexes: a case study of interactions between multiple electronic excited states. Coordination Chemistry Reviews,251: 351-361.
8. Figgis BN, 1967. The Magnatochemistry of Complex Compounds in Modern Coordination Chemistry. InterScience, New York.
9. Barry AL, 1980. Procedure for Testing Antimicrobial Agents in Agar Media. Theoretical Consideration in Antibiotics in Laboratory Medicine. 2nd Ed., Williams and Wilkins, London.
10. Barry AL, 1976. The Antibiotic Susceptibility Test: Principles and Practice. Lea and Febiger, Philadelphia.
11. Adhikary C, Mal D, Okamoto KI, Chaudhuri S, Koner S, 2006. Synthesis, characterization, X-ray structure and magnetic study of the azido adducts of tridentate (NNO) Schiff base copper (II) complexes. Polyhedron, 25: 2191-2197.
12. Stille JK, 1986. Angewandte Chemie International Edition in English. 25: 508.
13. Hughes MN, 1988. The Inorganic Chemistry of Biological Processes, 2nd Edn. John Wiley and Sons, 304.

14. Oshio H, Nihei M, Yoshida A, Nojiri H, Nakano M, Yamaguchi A, Karaki Y, Ishimoto H, 2005. A dinuclearMnIII-CuII single-molecule magnet. Chemistry - A European Journal, 11: 843-848.

15. Imbert D, Comby S, Chauvin AS, Bünzli JC, 2005. Lanthanide 8-hydroxyquinoline-based podates with efficient emission in the NIR range. Chemical Communications, 11: 1432-1434.

16. Mukherjee A, Dhar S, Nethaji M, Chakravarty AR, 2005. Ternary iron(II) complex with an emissive imidazopyridine arm from Schiff base cyclizations and its oxidative DNA cleavage activity. Journal of the Chemical Society Dalton Transactions,349-353.

17. Häner R, Hall J, 1997. The sequence-specific cleavage of RNA by artificial chemical ribonucleases.Antisense Nucleic Acid Drug Development, 7: 423-430.

18. Prasad KS, Kumar LS, Shekar SC, Prasad M, Revanasiddappa HD, 2011. Oxovanadium complexes with bidentate N, O ligands: Synthesis, characterization, DNA binding, nuclease activity and antimicrobial studies. Chemical Sciences Journal, 2011: CSJ-12.

19. Tsuji J,2004.Palladium Reagents and Catalysts: New Perspectives for the 21st Century.Wiley, Chichester (UK), Chapter 4.

20. Malleron JL, Fiaud JC, Legros JY,1997.Handbook of Palladium-Catalyzed Organic Reactions.Academic, San Diego.

21. Geary WJ, 1971. The use of conductivity measurements in organic solvents for the characterisation of coordination compounds. Coordination Chemistry Reviews, 7: 81-122.

22. Suberu H,2004. Preliminary studies of inhibitions in *Aspergillusflavus* with extracts of two lichens and Bentex-T fungicide. African Journal of Biotechnology,3**:**468–472.

23. El-HendawyAM, El-Kourashy AE, Shanab MM, 1992. Schiff base complexes of ruthenium(III), molybdenum(VI) and uranium(VI), and use of the former as catalytic organic oxidants. Polyhedron, 11: 523-530.

24. Chatt J, Leigh GJJ, 1968. Complexes of osmium, ruthenium, rhenium, and iridium halides with some tertiary monophosphines and monoarsines. Journal of Chemical Society A, 2636-2641.

25. Mahajan M, Saxena KN, Saxena CP, 1981. ESR study of Cu(II) complexes. Journal of Inorganic Nuclear Chemistry, 43: 2148-2151.

26. Dissouky AE, Rafaat LS, 1984. Metal chelates of heterocyclic nitrogen-containing ketones. XIV. Metal ion, anion and substituent effects on the enolization of mono-keto compounds. InorganicaChimicaActa,87: 213-222.

27. Nakamoto K, 1986. Infrared and Raman Spectra of Inorganic and Coordination Compounds, 4th Edn. John Wiley and Sons, New York.

28. Lever ABP, 1968. The electronic spectra of tetragonal metal complexes analysis and significance. Coordination Chemistry Reviews, 3: 119-140.

29. Tweedy BG, 1964. Plant extracts with metal ions as potential antimicrobial agents. Phytopathology, 55: 910-914.